This article has been accepted for inclusion in a future issue of this journal. Content is final as presented, with the exception of pagination.

Receding Horizon Adaptive Second-Order Sliding Mode Control for Doubly-Fed Induction Generator Based Wind Turbine

Carolina A. Evangelista, Alessandro Pisano, *Member, IEEE*, Paul Puleston, and Elio Usai, *Member, IEEE*

***Abstract*— In this paper, a novel adaptive second-order sliding mode technique to optimize the efficiency of certain types of variable-speed wind turbines is developed and analyzed. A revisited form of a recent adaptation algorithm is proposed to deal with the characteristics and control requirements of wind energy conversion systems (WECS), particularly model uncertainties and fast disturbances due to gusty wind effects. The revisited algorithm is based on appropriate receding horizon adaptation time windows rather than on fixed, adjacent, and nonoverlapping ones. This modification, which enhances the reactivity of the adaptation strategy against fast varying uncertainties, represents the main theoretical novelty of this paper. The proposed approach is successfully used to control a doubly fed induction-generator-based wind turbine topology proving its suitability for this application area. The novel adaptive controller is extensively assessed through computer simulations over a full-order realistic model of the WECS under study.**

***Index Terms*— Adaptive sliding mode control (SMC), conversion efficiency optimization, nonlinear control, second-order SM control (2-SMC), wind energy conversion systems (WECSs).**

I. Introduction

WIND energy conversion systems (WECSs) are one of the most significant renewable clean energy sources, and hence the development of dedicated controllers capable to improve their performance, lifetime, and conversion efficiency is essential for the progress of this ever-evolving technology [1]. However, WECSs are complex systems involving nonlinear dynamics with strongly coupled internal variables, external disturbances, and parameter uncertainties; consequently, advanced nonlinear control techniques are required to meet the challenge [2], [3].

Sliding Mode control (SMC) has proved to be an especially apt technique capable of coping with the aforementioned complex characteristics. In fact, since its origin [4], [5], SMC has evolved into a robust and powerful design technique for a wide range of applications [6]–[9]. The most distinguished aspect of SMC is the discontinuous nature of its control action, providing excellent system performance, which includes insensitivity to certain parameter variations, rejection of matching disturbances, and finite-time convergence.

However, in practice, direct application of such discontinuous control effort is not adequate for some actual plants. In addition, it can generate undesirable output chattering, which deteriorates the robustness of conventional SMC. To attenuate this problem, the concept of higher order sliding modes (SMs) was introduced and, specifically, several second-order sliding mode (2-SM) algorithms were presented [10]–[12]. Since then, a number of publications on 2-SM theory and applications have grown exponentially (see [13] and references therein for an overview).

Over the last decade, a number of interesting SMC solutions relying on adaptive mechanisms were presented. In [14] and [15], several adaptive first-order SMC algorithms were illustrated. The adaptive laws in [14] take advantage of the possibility of achieving an online estimate of the equivalent control, through low-pass filtering of the discontinuous control, which allows one to modulate the amplitude of the switching control component. To overcome the difficulty of selecting the time constant of the filter, in [15], a different mechanism was devised that exploits the size of the boundary layer to adjust the discontinuous control effort. As a result, the discontinuous gain is kept at the smallest level that allows a given SM accuracy. Subsequently, a great deal of research has been devoted to develop different forms of adaptive 2-SM algorithms. In [16], an adaptive version of the Super-twisting (ST) algorithm (see [10]) has been developed where time-varying gains are only allowed to grow. In [17], a Lyapunov-based variable-gain ST algorithm was developed where gains are

Manuscript received October 11, 2015; accepted February 6, 2016. Manuscript received in final form March 4, 2016. The work of C. A. Evangelista and P. Puleston was supported in part by the Universidad Nacional de La Plata (UNLP), in part by the European Union Seventh Framework Programme, Marie Curie Actions under Grant FP7-2011-IIF ACRES 299767/911767, in part by the Consejo Nacional de Investigaciones Científicas y Técnicas (CONICET), and in part by the Agencia Nacional de Promoción Científica y Tecnológica. The work of A. Pisano and E. Usai was supported in part by the Italian Ministry for Foreign Affairs and International Cooperation through the Project Robust Decentralised Estimation for Large-Scale Systems under Grant PGR00152 and in part by the Sardinia Regional Government through the Research Project Modeling, Control and Experimentation of Innovative Thermal Storage Systems and the Project Development, Design and Prototyping of Optimal Management and Control Systems for Micro-Grids under Grant CRP-60193 and Grant CRP-7733. Recommended by Associate Editor A. Zolotas.

C. A. Evangelista and P. Puleston are with the LEICI Instituto de Investigaciones en Electrónica, Control y Procesamiento de Señales, Facultad de Ingeniería, UNLP and CONICET, La Plata 1900, Argentina (e-mail: cae@ing.unlp.edu.ar; puleston@ing.unlp.edu.ar).

A. Pisano and E. Usai are with the Department of Electrical and Electronic Engineering, University of Cagliari, Cagliari 09123, Italy (e-mail: pisano@diee.unica.it; eusai@diee.unica.it).

Color versions of one or more of the figures in this paper are available online at http://ieeexplore.ieee.org.

Digital Object Identifier 10.1109/TCST.2016.2540539

1063-6536 © 2016 IEEE. Personal use is permitted, but republication/redistribution requires IEEE permission.
See http://www.ieee.org/publications_standards/publications/rights/index.html for more information.

This article has been accepted for inclusion in a future issue of this journal. Content is final as presented, with the exception of pagination.

adjusted on the basis of the currently measured states. The latter approach was applied in [18] and [19] to control different WECSs topologies with a generator similar to the one in this paper. Very good results were obtained regarding conversion efficiency and chattering reduction. However, the computation of the appropriate bounding functions could become difficult (as it was in [19] with the Multiple-Inputs Multiple-Outputs (MIMO) WECS) or even impractical if the system complexity is high.

Generalizing the methodology proposed in [14], the equivalent control principle has been exploited in [20]–[22] to develop adaptive ST algorithms. Particularly, the dual-layer adaptive concept of [22] provides a mechanism for adapting both gains of the ST, whose structure is slightly modified, and provides global convergence guarantees, which were not achieved in [20] and [21]. In parallel, generalizing the adaptation mechanism introduced in [15], adaptive versions of the ST algorithm were presented and experimentally verified in [23] and [24]. In contrast to our present proposal, a remarkable feature of such works is that they allow the uncertainty bounds not to be known *a priori*. On the other hand, limitations of those algorithms include the fact that the size of the guaranteed invariant boundary layer is not evaluated. Furthermore, only sliding variable dynamics having relative degree one can be considered since the ST algorithm is used, in contrast to the adaptive 2-SM control (2-SMC) approach of this paper where the relative degree can be one or two.

In [25], a continuous adaptive algorithm providing finite-time convergence to the 2-SM for a class of nonlinear systems of relative degree two having uncertain parameters was proposed. The twisting (TW) algorithm (see [10]) has also been developed in adaptive forms in [26]–[30]. While all the mentioned works feature certain structural differences, from a general viewpoint, the underlying Lyapunov-based adaptation principles are somewhat similar to those devised in [15] and [24], with the main exception of [26] where a hybrid adaptation rule based on an SM existence criterion has been employed. It should be mentioned that in this paper, we also take advantage of an SM existence criterion, which is, however, of completely different form compared with the one in [26].

A readily implementable and straightforward adaptive 2-SMC strategy was introduced in [31] to adjust the parameters of the TW algorithm. Instead of a Lyapunov-based gain adaptation (as in all the aforementioned works), this adaptation mechanism takes advantage of the inherent nature of the real (i.e., nonideal) SM regime, existing in actual systems operating at finite switching frequency. Its time-based adaptation policy simply depends on counting the zero crossings of the sliding variable during appropriate adaptation time windows. Then, the occurrence of the real SM behavior is verified by checking whether such a count is large enough according to an SM existence criterion. Like most of the existing adaptive 2-SMC schemes, the resulting adaptive controller is endowed with the capability of bidirectionally adjusting the discontinuous control gain, maintaining it at the minimum admissible level (rather than the worst case overconservative level, as in the fixed-gain SM). Moreover, without adding a great degree of extra complexity to the real-time computations, the proposed adaptation preserves the robustness of its parental fixed-gain counterpart, while allowing an effective response to unexpected changes in the working conditions and performance enhancement of the controlled system (e.g., stress alleviation and chattering reduction). This adaptive 2-SMC algorithm has been applied in [32] and [33] to adjust the parameters of the TW 2-SM algorithm [10] in robotic and automotive applications, respectively. Due to its computational simplicity, it proved to be specially suitable for implementation in standard microprocessor devices. In fact, it was experimentally verified in [32] by means of an industrial manipulator. More recently [34], the same logic combined with a switched adaptation algorithm (varying gains depending on the operating region) was applied to adjust the parameters of the Suboptimal 2-SM algorithm [12].

Driven by those encouraging results, the objective of this paper is to design, analyze, and establish the feasibility of time-based adaptive 2-SM techniques to control variable-speed WECSs, particularly doubly fed induction generator (DFIG)-based wind turbines. This type of turbines is an industry standard since the late 1990s, requiring only a slip power recovery fractional converter in the rotor (about 25%–30% of the total input mechanical energy), while the greater part of the power is fed to the grid directly from the stator. Efficiency increase and price reduction can be attained with such a configuration.

In this context, to face the stringent specifications of the control problem in the WECS scenario, where the uncertainties are subject to fast variations due to the wind effect, a revisited form of the time-based adaptation is sought. It is based on appropriate receding horizon adaptation time windows rather than on fixed, adjacent, and nonoverlapping ones, as in [32]–[34]. This modification, which enhances the reactivity of the adaptation strategy against fast varying uncertainties, represents the main theoretical novelty of this paper. Compared with [34], therefore, we are not using here the switched adaptation paradigm (where the controller parameters are adjusted according to the current operating region in the state space) and, furthermore, receding horizon adaptation time windows are used here.

Preliminary results of the application of this novel adaptive 2-SMC proposal to a simple Single-Input Single-Output WECS topology, based on a unidirectional DFIG and a dominant dynamic reduced-order model, were presented in [35].

Then, in this paper, the potential of the proposal for variable-speed WECSs is assessed by considering a versatile and comprehensive case study of a variable-speed DFIG-based topology with a bidirectional back-to-back converter drive in the rotor. The adaptive 2-SM MIMO controller design will be carried out by considering a simplified reduced-order mathematical model of the WECSs under study. The simulation studies, however, will be developed using the complete full-order model and in the presence of uncertainties, noise, and other perturbations.

The plan of this paper is as follows. A general introduction to WECSs is given in Section II. Then, the case study is

This article has been accepted for inclusion in a future issue of this journal. Content is final as presented, with the exception of pagination.

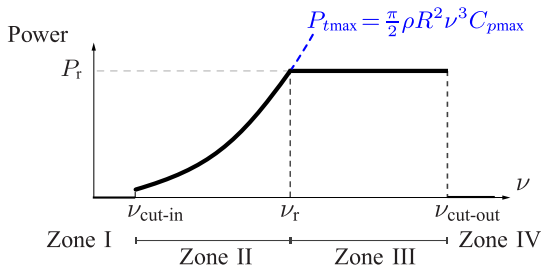

Fig. 1. Zones of operation for a wind turbine.

addressed in Section III, where the control objectives are stated and the sliding manifold design is developed. Afterward, Section IV presents the adaptive 2-SMC algorithm, together with the corresponding convergence proof. Section V presents some simulation results, and Section VI draws some conclusions and perspectives for next research.

II. Wind Energy Conversion System Basics

Typically, the operation of a DFIG-based wind turbine can be divided into four zones depending on the wind speed (see Fig. 1) [36]. For wind speeds lower than a given cut-in speed $\nu_{\text{cut-in}}$, Zone I, the wind is not strong enough to move the blades. Zone II, also known as partial-load zone, ranges between the cut-in speed and the rated one ν_r, and the control objective in such a zone is energy conversion efficiency maximization. Usually, in this zone, the pitch angle of the blades is fixed at its optimum and the generator speed is varied by means of the DFIG rotor electric drive. In Zone III, or full-load zone, which covers the interval from rated to cut-out wind speed $\nu_{\text{cut-out}}$, the controller must limit the power to its rated value. This can be accomplished by controlling the electric drive, by adjusting the pitch angle, or by a combination of both. In Zone IV, above $\nu_{\text{cut-out}}$, the turbine should be turned out of the wind to prevent damages, so the generated power is zero.

The mechanical power a real turbine can instantaneously extract from the wind, $P_t(t)$, is a fraction of the total available wind power, determined by the power coefficient of the turbine $C_p(\lambda(t), \beta(t))$ [36]

$$P_t(t) = 0.5\pi\rho R^2 C_p(\lambda(t), \beta(t))\nu^3(t) \tag{1}$$

where $\nu(t)$ is the wind speed, ρ is the air density, and R is the blade length. $C_p(\cdot)$ depends on the shape and geometrical dimensions of the turbine, and it is a nonlinear function of the pitch angle of the blades $\beta(t)$ and of the tip speed ratio $\lambda(t) = (\Omega_g(t)R/k_{gb}\nu(t))$, where $\Omega_g(t)$ is the angular speed of the generator rotor and k_{gb} is the transmission ratio of the speed multiplier (a rigid drive train is assumed). The curve $C_p(\lambda, \beta)$ presents a unique maximum, $C_{p\max} = C_p(\lambda_{\text{opt}}, \beta_{\text{opt}})$, corresponding to the condition of maximum power extraction [3], [36].

The nonlinear differential equation that describes the mechanical dynamics of the system is

$$\dot{\Omega}_g(t) = \frac{T_t(\nu(t), \Omega_g(t)) + T_g(i(t))}{J} \tag{2}$$

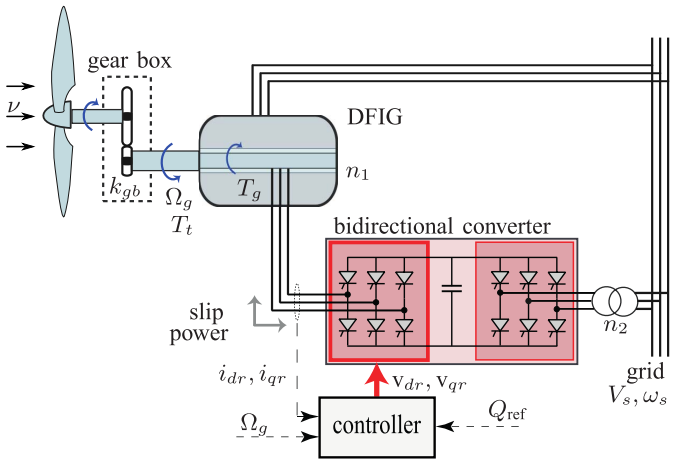

Fig. 2. Schematic variable-speed WECSs, based on a DFIG with a bidirectional back-to-back converter in the rotor.

where J is the inertia of the whole combined rotating parts, $T_t(\cdot) > 0$ is the torque exerted by the wind on the blades (referred to the high-speed side by the transmission ratio of the speed multiplier; see Appendix B), and $T_g(\cdot) < 0$ is the electrical resistant torque of the generator, which depends on the currents $i(t)$ of the DFIG [see (5) and (54)]. Note that friction terms are neglected and fixed pitch-angle operation at $\beta = \beta_{\text{opt}}$ is assumed. The expression of the turbine torque $T_t = P_t/\Omega_g$ becomes, after simple manipulations

$$T_t(\nu(t), \Omega_g(t)) = \frac{\pi\rho R^3}{2k_{gb}} C_t(\lambda(t))\nu^2(t) \tag{3}$$

where $C_t(\lambda) = C_p(\lambda, \beta_{\text{opt}})/\lambda$ is the torque coefficient modeled as $C_t(\lambda) = \sum_{i=0}^{3} c_i\lambda^i$ for some appropriate choice of coefficients c_i. From now on, the explicit dependence of the system variables on the time variable will be skipped for the sake of notation simplicity.

III. DFIG With Bidirectional Converter

The applicability of the proposed adaptive 2-SMC technique to DFIG-type WECSs is investigated by tackling a versatile DFIG topology, considering a bidirectional back-to-back converter in the rotor (see Fig. 2). This type of WECSs, largely used in variable-speed grid-connected applications, can operate in both subsynchronous and supersynchronous speed ranges. When operating supersynchronously, electrical power is fed to the grid through both the stator and the rotor, whereas for subsynchronous speeds, electrical power is injected into the rotor from the grid.

This configuration yields a multivariable system with two control inputs, i.e., the direct and quadrature rotor voltages, which makes it possible to pursue two independent objectives, for instance, active and reactive power control. In this work, a comprehensive control strategy is developed for operation in Zones II and III, without resorting to wind speed measurement.

A complete dynamical description of the system comprises five nonlinear differential equations (see Appendix B). By means of some geometrical considerations (relative alignment between the rotating frames and the spatial fluxes)

This article has been accepted for inclusion in a future issue of this journal. Content is final as presented, with the exception of pagination.

and a reasonable electric simplification (neglecting the stator resistance), a simplified third-order model can be obtained. This simplified description, whose variables are the direct and quadrature rotor currents and the mechanical rotation speed, is used for the control design, while the simulations for validation will be carried out using the full-order model. The reduced model is given by [37]

$$\begin{aligned}\frac{di_{qr}}{dt} &= -\left(\frac{L_m V_s}{L_{eq}} + \omega_s i_{dr}\right)\left(1 - \frac{p}{\omega_s}\Omega_g\right) - \frac{R_r L_s}{L_{eq}} i_{qr} + \frac{L_s}{L_{eq}} v_{qr} \\ \frac{di_{dr}}{dt} &= i_{qr}(\omega_s - p\Omega_g) - \frac{R_r L_s}{L_{eq}} i_{dr} + \frac{L_s}{L_{eq}} v_{dr} \end{aligned} \tag{4}$$

where v_{qr} and v_{dr} are the voltage control inputs and $L_{eq} = L_s L_r - L_m^2$, with L_m being the magnetizing inductance, and the third equation corresponds to (2), with the following expression for generator torque:

$$T_g(i_{qr}) = -\frac{3pL_m V_s}{2\omega_s L_s} i_{qr}. \tag{5}$$

A. Sliding Manifold Design

According to what has been stated above, two control objectives are tackled herein. The first one is to control the power extraction in Zones II and III, aiming to conversion efficiency optimization and power regulation, respectively, as shown in Fig. 1.

Given that it is assumed that no accurate wind speed information is available, the strategy for Zone II consists in indirectly attaining conversion efficiency maximization ($\lambda = \lambda_{\text{opt}}$) by tracking a time-varying optimum torque reference, which can be expressed as

$$T_{\text{opt}}(\Omega_g) = \frac{\pi \rho R^5 C_{p\max}}{2k_{gb}^3 \lambda_{\text{opt}}^3} \Omega_g^2 = k_o \Omega_g^2 \tag{6}$$

where $k_o = \pi \rho R^5 C_{p\max}/(2k_{gb}^3 \lambda_{\text{opt}}^3)$.

On the other hand, in Zone III, when the wind speed is high, the limitation of power to the rated value P_r can be performed by tracking a time-varying torque reference

$$T_r(\Omega_g) = \frac{P_r}{\Omega_g}. \tag{7}$$

The second control objective focuses on tracking an external reactive power reference in the stator, in order to contribute compensating for the grid power factor. The expression for the stator reactive power is [37]

$$Q_s(i_{dr}) = \frac{3pV_s^2}{2\omega_s L_s} - \frac{3pL_m V_s}{2L_s} i_{dr}. \tag{8}$$

Then, the following two sliding variables are defined:

$$\sigma_1 = T_{\text{ref}} + T_g = T_{\text{ref}}(\Omega_g) - \frac{3pL_m V_s}{2\omega_s L_s} i_{qr} \tag{9}$$

$$\sigma_2 = Q_{\text{ref}} - Q_s = Q_{\text{ref}} + \frac{3pL_m V_s}{2L_s}\left(i_{dr} - \frac{V_s}{\omega_s L_m}\right) \tag{10}$$

where Q_{ref} is the external time-varying reference for the reactive power and $T_{\text{ref}}(\Omega_g)$ is the torque reference

$$T_{\text{ref}}(\Omega_g) = \begin{cases} k_o \Omega_g^2, & \Omega_g \le \Omega_{g_{\text{rated}}} \\ \dfrac{P_r}{\Omega_g}, & \Omega_g > \Omega_{g_{\text{rated}}}. \end{cases} \tag{11}$$

By virtue of (2) and (4)–(8), the time derivatives of the sliding variables take the form

$$\dot{\sigma}_1(t) = \frac{dT_{\text{ref}}}{dt} - \frac{dT_g}{dt} = \frac{T_t + T_g}{J}\frac{dT_{\text{ref}}}{d\Omega_g} - \frac{3pL_m V_s}{2\omega_s L_s}\frac{di_{qr}}{dt} \tag{12}$$

$$\dot{\sigma}_2(t) = \dot{Q}_{\text{ref}} - \frac{dQ_s}{dt} = \dot{Q}_{\text{ref}} + \frac{3pL_m V_s}{2L_s}\frac{di_{dr}}{dt}. \tag{13}$$

Note that the control inputs $u_1 = -v_{qr}$ and $u_2 = v_{dr}$ enter into the right-hand side of (12) and (13) through the derivatives of the electrical currents, given in (4). Differentiating further (12) and (13) yields two expressions, which can be written in the form

$$\ddot{\sigma}_j(t) = f_j(\Omega_g, i_{qr}, i_{dr}, u_j, t) + g_j \dot{u}_j, \quad j = 1, 2 \tag{14}$$

highlighting the affine and decoupled dependence of each $\ddot{\sigma}_j$ on the corresponding control derivative $\dot{u}_j$. The 2-SMC design requires that the following inequalities hold for some constants G_{mj}, G_{Mj}, and F_j, $j = 1, 2$:

$$0 < G_{mj} \le g_j \le G_{Mj}; \quad |f_j| \le F_j. \tag{15}$$

To obtain appropriate theoretical bounds, the following expressions can be straightforwardly found by differentiation and adequate rewriting (arguments of functions f_j and g_j and time-varying signals are omitted for brevity):

$$\begin{aligned} f_1 = &-\frac{3p^2 L_m V_s}{2\omega_s L_s J}\left(i_{dr} + \frac{L_m V_s}{\omega_s L_{eq}}\right)\varphi_1 \\ &+ \frac{d^2 T_{\text{ref}}}{dt^2} + \frac{3pL_m V_s(\omega_s - p\Omega_g)}{2\omega_s L_s} \\ &\times \left(\frac{L_s}{L_{eq}} v_{dr} - \frac{R_r L_s}{L_{eq}} i_{dr} + (\omega_s - p\Omega_g) i_{qr}\right) + \frac{3pL_m R_r V_s}{2\omega_s L_{eq}} \\ &\times \left[\left(\frac{L_s}{L_{eq}} v_{qr} - \frac{L_m V_s}{L_{eq}} + \omega_s i_{dr}\right)\left(1 - \frac{p\Omega_g}{\omega_s}\right) - \frac{R_r L_s}{L_{eq}} i_{qr}\right] \end{aligned} \tag{16}$$

where $\varphi_1 = (T_t - (3pL_m V_s/2\omega_s L_s) i_{qr})$ and the second time derivative of T_{ref} depends on the zone of operation

$$\frac{d^2 T_{\text{ref}}}{dt^2} = \begin{cases} \dfrac{2k_o}{J^2}\varphi_1 + \dfrac{2k_o \Omega_g}{J}\varphi_2, & \Omega_g \le \Omega_{g_{\text{rated}}} \\ \dfrac{2P_r}{J^2 \Omega_g^3}\varphi_1 - \dfrac{P_r}{J\Omega_g^2}\varphi_2, & \Omega_g > \Omega_{g_{\text{rated}}} \end{cases} \tag{17}$$

with

$$\begin{aligned} \varphi_2 = &\frac{\rho \pi R^3}{2k_{gb}}\left[\left(2c_0 \nu + \frac{c_1 R \Omega_g}{k_{gb}} - \frac{c_3 R^3 \Omega_g^3}{k_{gb}^3 \nu^2}\right)\dot{\nu}\right. \\ &\left. + \frac{\varphi_1}{J}\left(\frac{c_1 R \nu}{k_{gb}} + \frac{2c_2 R^2 \Omega_g}{k_{gb}^2} + \frac{3c_3 R^3 \Omega_g^2}{k_{gb}^3 \nu}\right)\right] \end{aligned} \tag{18}$$

$$\begin{aligned} f_2 = &\ddot{Q}_{\text{ref}} - \frac{3p^2 L_m V_s}{2L_s J}\varphi_1 - \frac{3pL_m L_s V_s}{2L_{eq}^2} v_{dr} \\ &- \frac{3pL_m V_s}{L_{eq}}(\omega_s - p\Omega_g)\left[\frac{L_m V_s(\omega_s - p\Omega_g)}{2\omega_s L_s} + R_r i_{qr}\right] \\ &- \frac{3pL_m V_s}{2} i_{dr}\left[\frac{(\omega_s - p\Omega_g)^2}{L_s} - \frac{R_r^2 L_s}{L_{eq}^2}\right] \\ &+ \frac{3pL_m V_s}{2L_{eq}}(\omega_s - p\Omega_g) v_{qr} \end{aligned} \tag{19}$$

This article has been accepted for inclusion in a future issue of this journal. Content is final as presented, with the exception of pagination.

TABLE I
MAXIMUM RANGES FOR THE UNCERTAIN TIME-VARYING SIGNALS

ν:	$[6\,;\,12]$ (m/s)	i_{qr}:	$[-80\,;\,80]$ (A)
$\dot{\nu}$:	$[-0.5\,;\,0.5]$ (m/s^2)	i_{dr}:	$[\ 0\,;\,40]$ (A)
$\ddot{\nu}$:	$[-0.1\,;\,0.1]$ (m/s^3)	v_{qr}:	$[-300\,;\,300]$ (V)
Ω_g:	$[0.7\Omega_s\,;\,1.3\Omega_s]$ (rad/s)	v_{dr}:	$[\ 0\,;\,30]$ (V)

$$g_1 = \frac{3pL_mV_s}{2\omega_s L_{eq}} \tag{20}$$

$$g_2 = \frac{3pL_mV_s}{2L_{eq}}. \tag{21}$$

Then, to compute the bounding constants in (15), a worst case analysis has been performed, considering maximum admissible intervals for the time-varying signals entering (16)–(21) (see Table I).

Assuming uncertainties and other possible external disturbance effects as well yields the following conservative theoretical bounds:

$$F_1 = 1.40316 \times 10^8; \quad F_2 = 5.86104 \times 10^{10} \tag{22}$$

$$G_{m1} = 1.4754 \times 10^3; \quad G_{M1} = 2.2131 \times 10^3 \tag{23}$$

$$G_{m2} = 5.5620 \times 10^5; \quad G_{M2} = 8.3430 \times 10^5. \tag{24}$$

IV. ADAPTIVE SECOND-ORDER SLIDING MODE DESIGN

At this point, it is convenient to use a unified representation to write down each equation of second-order nonlinear uncertain system (14), which, respectively, governs the dynamics of the sliding variables σ_1 and σ_2. They take the following form:

$$\begin{cases} \dot{z}_1^j(t) = z_2^j(t) \\ \dot{z}_2^j(t) = f_j + g_j v_j(t) \end{cases} \qquad j = 1, 2 \tag{25}$$

where $z_1^j(t) = \sigma_j(t)$, $v_j(t) = \dot{u}_j(t)$ is the auxiliary control signal, and $f_j(\cdot)$ and $g_j(\cdot)$ are uncertain functions satisfying the inequalities stated in (15).

The two subsystems (25) will be now treated in a unified way, and hence the subscript and superscript j in the corresponding functions and variables will be dropped for the sake of simplicity. Therefore, from now on, we let $z_1(t) = \sigma(t)$, and (25) and (15) will be represented, respectively, as

$$\begin{cases} \dot{z}_1(t) = z_2(t) \\ \dot{z}_2(t) = f(\cdot) + g(\cdot)v(t) \end{cases} \tag{26}$$

$$0 < G_m \le g \le G_M; \quad |f| \le F. \tag{27}$$

To stabilize in finite time the uncertain auxiliary systems (26) and (27), the following discontinuous algorithm, called the Suboptimal algorithm, was proposed in [12]:

$$v(t) = \dot{u}(t) = -\alpha(t)V\ \mathrm{sgn}(z_1 - z_{1M}/2) \tag{28}$$

$$\alpha(t) = \begin{cases} \alpha^* & \text{if } \left(z_1 - \dfrac{z_{1M}}{2}\right)(z_{1M} - z_1) > 0 \\ 1 & \text{otherwise} \end{cases} \tag{29}$$

where z_{1M} is the last extremal value of z_1 (more precisely, the most recent local maximum, minimum, or horizontal flex point of the sliding variable, which can be evaluated with sufficient precision using measurements of z_1 only [38]), and α^* and V are tuning constants to be selected in accordance with the next inequalities

$$\alpha^* \in (0, 1] \cap \left(0, \frac{3G_m}{G_M}\right) \tag{30}$$

$$V > \frac{F}{G_m}\Phi, \quad \Phi = \max\left\{\frac{1}{\alpha^*}, \frac{4G_m}{3G_m - \alpha^* G_M}\right\}. \tag{31}$$

Such a constant-gain controller is modified by implementing a time-based adaptation mechanism, which properly adjusts the gain parameter V, now denoted by $V_{tb}(t)$, thereby changing (28) into

$$v(t) = \dot{u}(t) = -\alpha(t)V_{tb}(t)\ \mathrm{sgn}(z_1 - z_{1M}/2). \tag{32}$$

The adaptation method that will be implemented is inspired by the one introduced in [31] for the TW 2-SM algorithm, and that was tailored to the Suboptimal algorithm in [34]. It is worth noting that in this paper, we develop a different form of adaptation mechanism compared with that suggested in [34].

The basis of the adaptation logic is a suitable *SM existence criterion*. Receding horizon time intervals of fixed length T are considered of the form

$$\mathcal{T}_k \equiv [kT_a - T, kT_a] \quad k = k^*, k^* + 1, \ldots \tag{33}$$

where $T_a \ll T = k^*T_a$, $k^* \in \mathbb{N}$. T_a is the adaptation period of the gain-adjusting mechanism and T is the adaptation window. At the end of every interval $\mathcal{T}_k$, the number of zero crossings of the quantity

$$\omega(t) = z_1(t) - z_{1M}/2 \tag{34}$$

during such an interval is computed. Note that function $\omega(t)$ appears as an argument of the sign function in the Suboptimal algorithm control law (32), and hence, when the corresponding number of zero crossings is sufficiently large, it means that a real SM behavior occurs in a small vicinity of the sliding manifold. In turns, this implies that the control value is large enough to counteract the actual uncertainties. Thus, if the SM existence criterion is fulfilled, it is sensible to diminish the control gain at the end of the time interval. On the other hand, when the SM existence criterion is violated, then the control gain is increased. Upper and lower saturation thresholds to the control gain $V_{tb}(t)$ are also taken into account.

The time-based adaptation works as follows. The piecewise constant gain $V_{tb}(t)$ is defined according to

$$V_{tb}(t) = V_M^k, \quad t \in [kT_a, (k+1)T_a). \tag{35}$$

The amplitude parameter V_M^k is adjusted according to

$$V_M^i = V_0, \quad i = 0, 1, 2, \ldots, k^* - 1$$

$$V_M^{k+1} = \begin{cases} \max\left(V_M^k - \Lambda T_a, V_{\min}\right) & \text{if } N_{sw}^k(\omega) \ge N^* \\ \min\left(V_M^k + \Gamma T_a, V_{\max}\right) & \text{if } N_{sw}^k(\omega) < N^* \end{cases} \quad \text{for } k \ge k^* \tag{36}$$

where $N_{sw}^k(\omega)$ is the number of sign commutations of $\omega(t)$ in the interval $\mathcal{T}_k$ and N^* is an appropriate integer threshold. Roughly speaking, at the end of each time interval $\mathcal{T}_k$, we decrement the time-based control magnitude $V_{tb}(t)$ stepwise

This article has been accepted for inclusion in a future issue of this journal. Content is final as presented, with the exception of pagination.

by ΛT_a if the SM existence criterion is fulfilled; otherwise, we increment it stepwise by ΓT_a. The adaptation logic also includes lower and upper bounds for the control magnitude [$V_{\min}$ and $V_{\max}$, respectively, the latter being a value fulfilling $V_{\max} > (F/G_m)\Phi$, where Φ is defined in (31)]. Finally, V_0 is an arbitrary nonnegative initial value that can be selected smaller than $V_{\max}$. Note that the uncertainty bounds in (22)–(24) affect only the computation of the $V_{\max}$ parameter.

We preliminarily recall a useful lemma, which will be invoked within the convergence proof of the algorithm.

Lemma 1 [33]: Consider the second-order auxiliary system (26) with the Suboptimal algorithm as the control law, and let $N_{sw}^k(\omega)$ be the number of zero crossings of $\omega = z_1 - z_{1M}/2$ during the time interval $\mathcal{T}_k$ of length T. If the condition

$$N_{sw}^k(\omega) \geq 3 \tag{37}$$

is satisfied and, additionally, there is $a_1 > 0$ such that $|\ddot{z}_1(t)| \leq a_1 \ \forall t \in \mathcal{T}_k$, then there exist constants ρ_1 and ρ_2, independent of T, such that the next inequalities hold

$$|z_1(t)| \leq \rho_1 T^2 \quad |z_2(t)| \leq \rho_2 T \quad \forall t \in \mathcal{T}_k. \tag{38}$$

Proof of Lemma 1: See [33].

Rewrite the last equation of (25) as follows:

$$\dot{z}_2(t) = g[\eta(t) + \upsilon(t)], \quad \eta(t) = \frac{f}{g}. \tag{39}$$

We assume that a positive constant P exists such that

$$\left|\frac{d}{dt}\eta(t)\right| \leq P, \quad t \geq 0. \tag{40}$$

We are now in a position to state the next theorem.

Theorem 1: Consider system (26). Assume that the uncertain functions $f(\cdot)$ and $g(\cdot)$ satisfy the inequalities (27). Apply the time-based adaptive Suboptimal control law (29)–(32), (35), and (36) with (31) specified with $V = V_{\max}$ and

$$\Lambda > 0, \quad \Gamma > \Lambda + 3P, \quad N^* \geq 3. \tag{41}$$

Then, with large enough parameters T_a and T, the next relations are achieved after a finite-time transient for some positive constants b_1 and b_2

$$|z_1(t)| \leq b_1 T^2, \quad |\dot{z}_2(t)| \leq b_2 T. \tag{42}$$

Proof of Theorem 1: See Appendix A.

Remark 1: It is worth remarking that the complicated relations (16)–(21) do not contribute to the real-time computations. In fact, they represent the drift and gain terms of the sliding variable dynamics (14), and such functions are used only offline for computing the constants appearing in (22)–(24). The online computations to derive the actual value of the control input to be applied, to be made every T_a, are limited to the computation of the last extremal value z_{1M} (which just requires few subtractions and multiplications as explained in [38]), the computation of the current value of the gain V_M^{k+1} according to (36), and the computation of the current value of the control input time derivative according to (29) and (32), and finally the discrete-time integration (e.g., by the Euler method). Thus, the computational burden of the proposed algorithm turns out to be particularly simple.

A. Practical Tuning of the Algorithm

Some guidelines for finding an effective tuning of the adaptive 2-SM controller parameters are given. This is useful, on one hand, because there is a large freedom in selecting their values, and on the other hand, because the restriction $\Gamma > \Lambda + 3P$ in (41) is usually highly conservative. Thus, a practically oriented tuning procedure is helpful as a viable way to obtain the best performance from the proposed adaptive control algorithm.

In practice, due to discretization, measurement noise, and/or actuator bandwidth limitations, the time interval between two successive adjustments of the control input has a lower threshold. According to this unavoidable implementation constraint, the parameter T_a has to be chosen not less than such a threshold.

Then, the pair (T, N^*) should be selected jointly. This is done by first choosing the interval length T as an integer multiple of T_a and then making an experimental (or simulative) test using the fixed-gain version of the controller and inspecting the actual average number of switches of the quantity $\omega(t)$ along time windows of length T. This observed average value has then to be reduced (e.g., dividing it by two) to derive N^*. The rationale for this procedure is that the average switching frequency of the sliding variable will decrease when the magnitude of the discontinuous controller gain is diminished.

The Λ parameter is chosen arbitrarily, being convenient to use relatively small values to avoid an excessively nervous adaptation of the gain. Finally, the parameter Γ must formally fulfill the inequality in (41), which is, however, unsuitable since the parameter P is usually highly conservative. Γ should be chosen large enough to allow a prompt restoring of the practical SM condition when it is lost. In this sense, selecting its value between five and ten times the value of Λ represents a reasonable choice.

V. Simulation Results

In this section, the unified notation adopted in Section IV is dropped. Thus, the parameters V_0, $V_{\max}$, $V_{\min}$, Λ, Γ, and N^* from (36) associated with sliding variable σ_j, $j = 1, 2$, and its corresponding controller u_j will now be explicitly denoted by $V_{0,j}$, $V_{\max,j}$, $V_{\min,j}$, Λ_j, Γ_j, and N_j^*, respectively.

The performance of the proposed adaptive 2-SM control system is assessed via computer simulations. The simulation runs correspond to 10 min of system operation, using the wind profile shown in Fig. 3, which spans over Zones II and III.

The simulated system is a three-bladed horizontal-axis WECSs based on a DFIG with a bidirectional converter and a rated power of 37 kW. Its full-order model is used in this section (the model and nominal parameters can be found in Table II of Appendix C). In addition, a friction torque disturbance was applied at $t \geq 300$ s, which is shown in Fig. 4 (top), and time-varying fluctuations of the grid line voltage and frequency have been considered [see Fig. 4 (bottom)]. All system parameters have also been subject to variations up to 20% with respect to their nominal values.

This article has been accepted for inclusion in a future issue of this journal. Content is final as presented, with the exception of pagination.

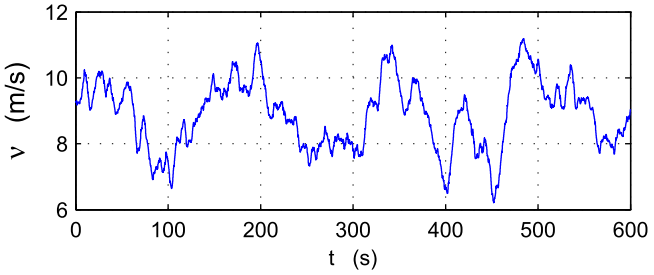

Fig. 3. Wind speed profile.

The plan of the simulation analysis is as follows. First, in Section V-A, a comparison between the fixed-gain 2-SM controllers (28) and (29) and the adaptive version proposed herein will be presented in the absence of noise. Subsequently, in Section V-B, significant implementation issues such as the presence of measurement noise and the sensitivity of the adaptive controller against the chosen sampling period will be investigated.

A. Adaptive Versus Fixed-Gain 2-SM Controllers

To compare both controllers, the values of all the parameters were determined in the first place. The computation of the fixed-gain parameters (V_1, α_1^*, V_2, and α_2^*) based on the theoretical bounds introduced in (22)–(24) provides extremely large values, not feasible for implementation as they will cause unacceptable chattering in the fixed-gains realization of the controller. After further heuristic refinement, the following parameters, suitable for practical use, have been employed:

$$\alpha_1^* = 0.54; \quad V_1 = 300. \quad \alpha_2^* = 0.54; \quad V_2 = 30. \tag{43}$$

With regard to the proposed adaptive 2-SM controller, the explicit expressions of the control law, where $u_1 = -v_{qr}$ and $u_2 = v_{dr}$, are as follows:

$$\begin{aligned} \dot{u}_j(t) &= -\alpha_j^*(t) V_{tb,j}(t)\,\mathrm{sgn}(\sigma_j - \sigma_{jM}/2) \\ V_{tb,j}(t) &= V_{Mj}^k, \quad t \in [kT_a, (k+1)T_a) \\ V_{Mj}^i &= V_{0,j} \quad i = 0, \ldots, k^* - 1 \\ V_{Mj}^{k+1} &= \begin{cases} \max\left(V_{Mj}^k - \Lambda_j T_a, V_{\min,j}\right) & \text{if } N_{sw}^k(\omega_j) \geq N_j^* \\ \min\left(V_{Mj}^k + \Gamma_j T_a, V_{\max,j}\right) & \text{if } N_{sw}^k(\omega_j) < N_j^* \end{cases} \\ & \qquad \text{for } k \geq k^* \end{aligned} \tag{44}$$

where $N_{sw}^k(\omega_j)$ is the number of sign commutations of $\omega_j(t) = \sigma_j - (\sigma_{jM}/2)$ in the intervals $\mathcal{T}_k \equiv [kT_a - T, kT_a]$, as defined in (33). The practical tuning procedure previously outlined in Section IV-A has been followed and its parameters were finally set as follows:

$$\begin{aligned} T_a &= 1 \text{ ms}; \quad T = 200T_a \\ N_1^* &= 6; \quad \Lambda_1 = 1.2; \quad \Gamma_1 = 9 \\ V_{\max,1} &= V_1; \quad V_{\min,1} = 0.1; \quad V_{0,1} = 100 \\ N_2^* &= 4; \quad \Lambda_2 = 0.2; \quad \Gamma_2 = 2.3 \\ V_{\max,2} &= V_2; \quad V_{\min,2} = 0.1; \quad V_{0,2} = 10 \end{aligned} \tag{45}$$

where $T_a = 1$ ms was obtained from practical considerations in accordance with the response time allowed by the measurement and actuator subsystems.

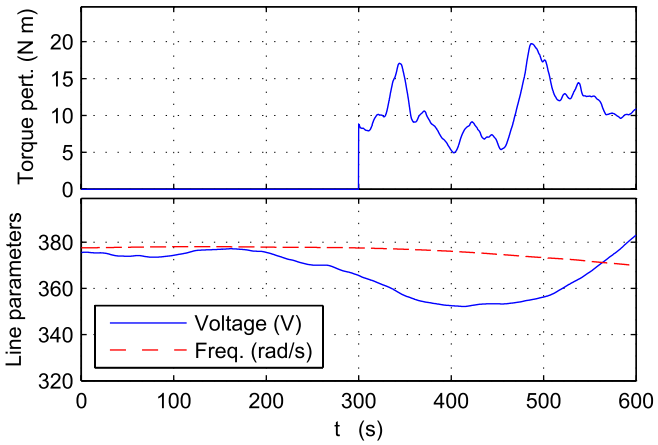

Fig. 4. Top: variations of the grid line voltage and line frequency. Bottom: torque disturbance.

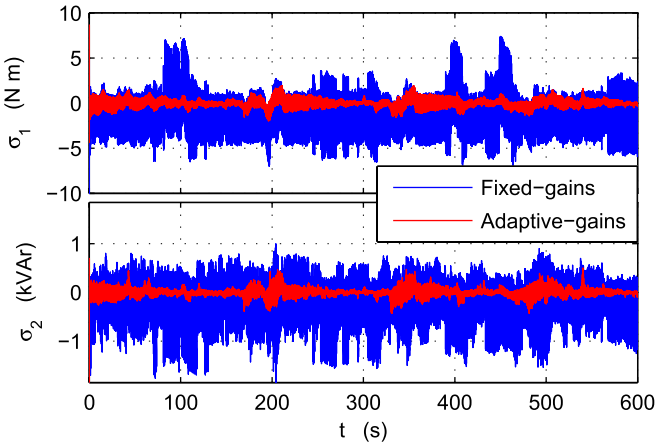

Fig. 5. Sliding variables with the fixed-gain controller and the adaptive controller.

The time evolution of the sliding variables σ_1 and σ_2 obtained using the fixed-gain and adaptive controllers are depicted in Fig. 5. The fixed-gain and the time-based adaptive controllers achieved the desired objectives, steering to and confining the sliding variables within a vicinity of zero in both cases. However, a significant chattering reduction can be appreciated when the adaptive controller is employed.

Note that tuning the gains large enough to deal with the uncertainties and disturbances in a wide operating range has another negative effect on the fixed-gain controller performance, besides the aforementioned output chattering. This is the generation of severe mechanical efforts that can be inferred from its broad torque variations in Fig. 6.

Counteracting the rate of variation of the generator torque is of paramount importance to increase the lifetime of WECSs. Evidently, this could be attained with the fixed-gain controller by reducing its gains, but at the expense of narrowing its robustness region and with the incorporation of an additional action into the control law, responsible to drive the system inside that region. On the other hand, without range reduction, it can be observed that the adaptive 2-SM controller provides in fact a remarkable attenuation of the generator torque vibrations (see the details in Fig. 6).

This article has been accepted for inclusion in a future issue of this journal. Content is final as presented, with the exception of pagination.

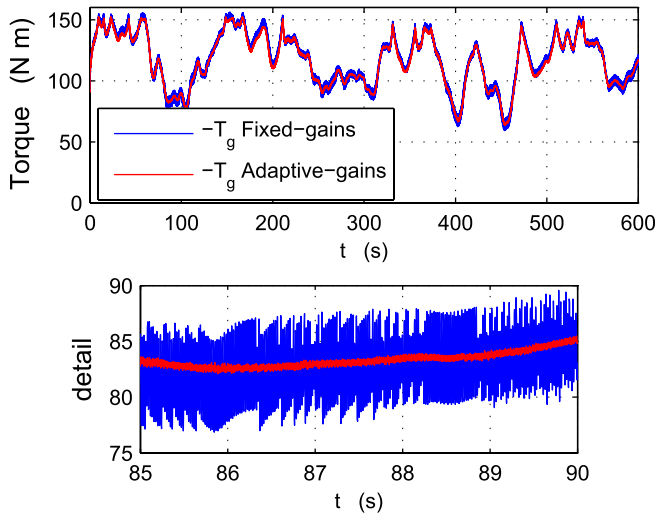

Fig. 6. Torque with the fixed-gain controller and the adaptive controller for whole time range (top) and a detail (bottom).

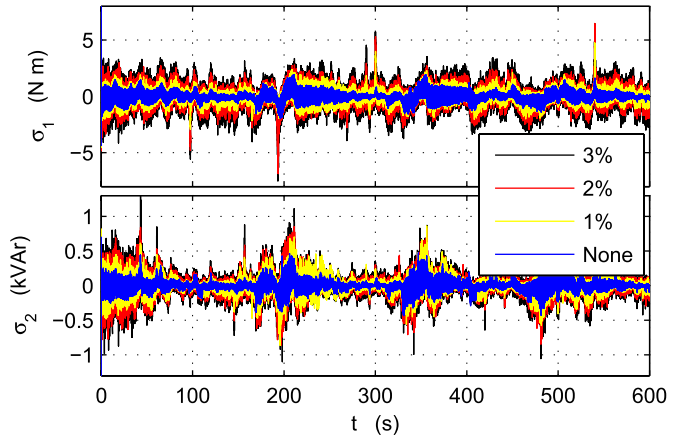

Fig. 7. Sliding variables when different magnitudes of measurement noise are considered.

B. Noise and Discretization Effects

To validate the performance of the adaptive Suboptimal controller in a more realistic scenario, measurement noise has been included in a further series of tests. Particularly, different simulation runs have been made by varying the noise level from 1% to 3% of the measurement range. Fig. 7 depicts the obtained time evolutions of the sliding variables σ_1 and σ_2, showing the corresponding progressive deterioration of the sliding accuracy when the measurement noise is considered. A continuous dependence of the sliding accuracy on the noise magnitude is observed.

Fig. 8 depicts the actual and reference profiles of the generator torque [Fig. 8 (top)] and the stator reactive power [Fig. 8 (bottom)], showing that very good tracking is attained by the proposed controller also in the presence of noise. It is worth pointing out a slight deterioration of the generator torque tracking accuracy at $t \geq 300$ (i.e., when the friction torque is added). The tracking precision, however, remains satisfactory. Short transient peaks can be seen in the Q_s profile at the transition times between operating zones.

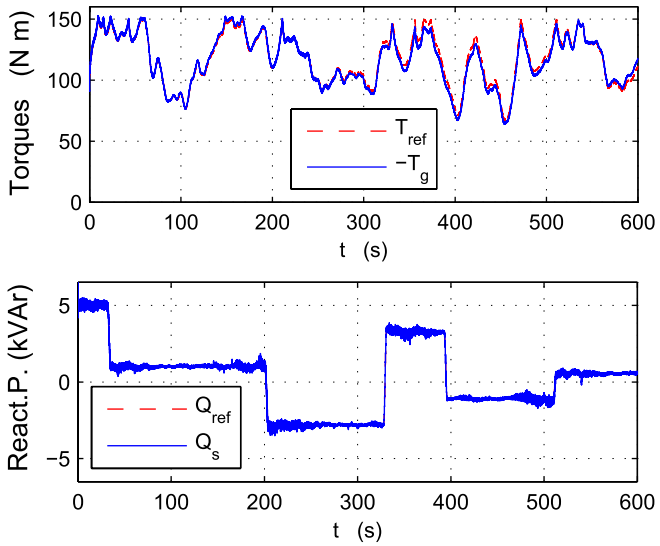

Fig. 8. Top: actual and reference generator torques. Bottom: actual and reference stator reactive powers. (Simulations considering measurement noise.)

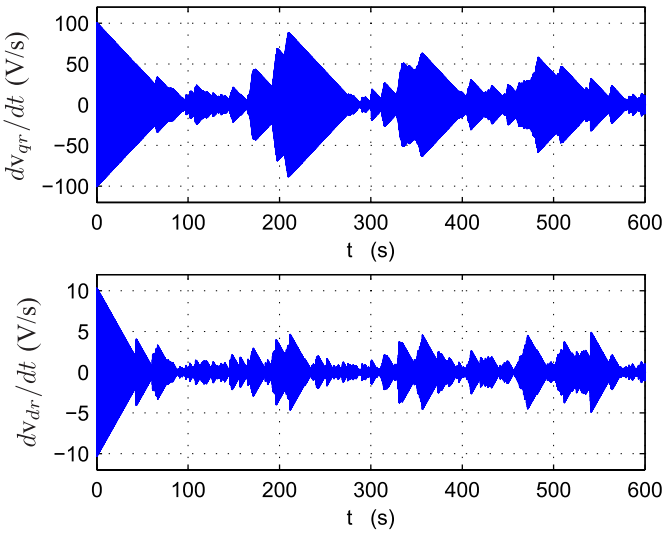

Fig. 9. Control voltages derivatives: $\dot{u}_1 = (dv_{qr}/dt)$ (top) and $\dot{u}_2 = (dv_{dr}/dt)$ (bottom). (Simulations considering measurement noise.)

Fig. 9 displays the control voltage derivatives $\dot{u}_1 = (dv_{qr}/dt)$ [Fig. 9 (top)] and $\dot{u}_2 = (dv_{dr}/dt)$ [Fig. 9 (bottom)], showing the continuous adjustment of their magnitude provided by the adaptive 2-SMC scheme to face the variation of the uncertain drift and control gain terms. Fig. 10 displays the corresponding applied control voltages $u_1 = v_{qr}$ and $u_2 = v_{dr}$, which appear to be immune to chattering.

The sensitivity of the adaptive controller against the choice of the sampling period T_a is investigated next. Since the proposed adaptation mechanism counts the number of sign commutations of the sliding variable, it is expected that in the presence of noise selecting a too small value for T_a will yield the failure of the adaptation. A related analysis was made in [39], where the sensitivity of the TW algorithm to the presence of noise was under investigation and led

This article has been accepted for inclusion in a future issue of this journal. Content is final as presented, with the exception of pagination.

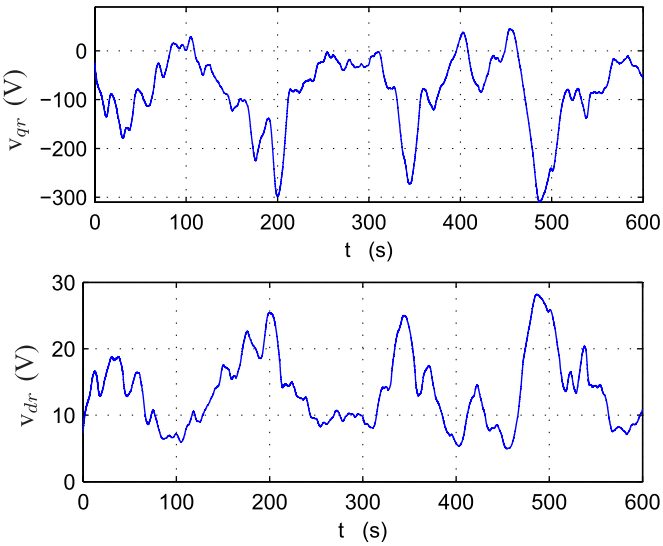

Fig. 10. Control voltages: $u_1 = v_{qr}$ (top) and $u_2 = v_{dr}$ (bottom). (Simulations considering measurement noise.)

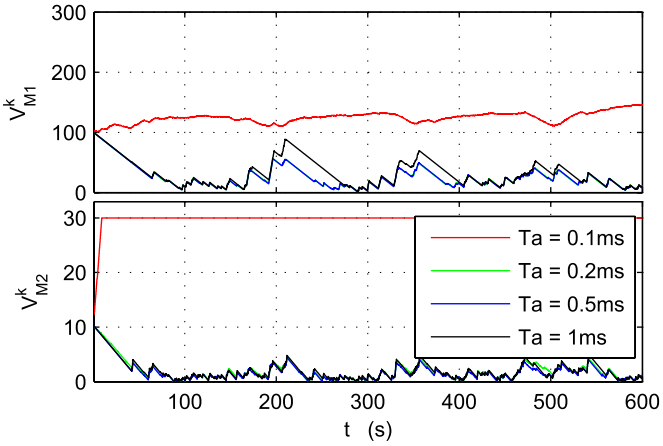

Fig. 11. Adjustments of the amplitude parameter of the gains, $V_{tb,1}(t) = V^k_{M1}$ and $V_{tb,2}(t) = V^k_{M2}$, for smaller adaptation periods of the gains T_a with measurement noise.

to the important result that the sampling period should be selected proportional to the square root of the measurement noise magnitude since accuracy deterioration is observed using smaller values. The same result readily translates to the present scenario, since the Suboptimal algorithm is homogeneous and the proposed adaptation is based on the sign of the sliding variable (in analogy with the TW controller). The proportionality constant is hard to compute and trial and error is needed in practice to properly tune the T_a parameter. Next simulations clearly show this fact. Fig. 11 depicts the adaptive gains corresponding to different tests where reduced values for T_a compared with the value $T_a = 1$ ms used in all the previous simulations were used. It can be seen that the smallest value $T_a = 0.1$ ms leads to the failure of the gain adaptation in both the torque and reactive power control loops.

Overall, all presented tests have shown that the proposed adaptation mechanism is a practical solution, rather simple and easy to implement, to address the high performance control of a WECS under significant uncertainty effects and bring considerable improvements compared with the corresponding fixed-gain counterpart.

VI. Conclusion

A robust controller setup for power conversion maximization and reactive power regulation of wind turbines was designed. To this end, an existing adaptive 2-SMC scheme has been revisited in order to deal with quickly varying disturbances (such as those present in WECSs) and its theoretical foundation was demonstrated. After thorough simulation tests, the novel time-based adaptive WECS controller has shown satisfactory performance and robustness attesting not only the potential applicability of this combined control technique in the area of wind energy technology, but also its general applicability to nonlinear systems subjected to fast varying uncertainty sources.

The critical issue of the selection of the T_a parameter should be kept in mind while tuning the control system, and particularly, the variable measurement step strategy suggested in [39], suitably tailored to the present scenario, could be usefully implemented to further robustify the proposed controller. This issue will be investigated in our next research.

This research is the preliminary stage of a broader project aiming to implement and compare several adaptive 2-SM controllers in a real small-scale wind turbine (10–60 kW) to optimize energy capture and extend its service life.

Appendix A
Proof of Theorem 1

Unlike the initial conditions already belonging to a close vicinity of the origin of the z_1Oz_2 plane, during the initial transient, there are no frequent sign commutations of $\omega(t)$, and hence, the time-based magnitude $V_{tb}(t)$ will start increasing from its initial value V_0 and two possible scenarios can arise.

In one of them, $V_{tb}(t)$ will reach the maximum value $V_{\max}$ and then keep constant. Then, according to the convergence properties of the fixed-gain version of the Suboptimal algorithm, the resulting trajectories will start to converge toward the origin.

While approaching the origin, the contraction condition $|z_{1M,h+1}| \leq \gamma\,|z_{1M,h}|$ ($\gamma < 1$) is enforced by the Suboptimal algorithm, and the frequency of the sign commutations of $\omega(t)$ will progressively increase. Theoretically, the frequency of sign commutations of $\omega(t)$ tends to infinity while approaching the origin. Hence, the real-sliding criterion (37) is fulfilled at some $k = M_1$, and the stepwise reduction of V^k_M will be then activated starting from the end of the time interval $\mathcal{T}_{M_1}$.

In the other possible, and more favorable, scenario, $V_{tb}(t)$ will be growing during the initial transient, but the real-sliding criterion (37) will be already achieved before that $V_{tb}(t)$ reaches the maximum value $V_{\max}$. Also in this case, the stepwise reduction of V^k_M will be activated starting from the end of some time interval $\mathcal{T}_{M_1}$.

The gain dominance condition (31) can be specialized to a restricted time interval $\mathcal{T}_k$ as follows:

$$V_{\max} > \Phi N_k, \quad N_k = \sup_{t \geq \mathcal{T}_k} |\eta(t)| \leq F/G_m. \tag{46}$$

This article has been accepted for inclusion in a future issue of this journal. Content is final as presented, with the exception of pagination.

By relying on the fact that $N_{sw}^{M_1}(\omega) \geq N^*$, there is $\tau_1 \in \mathcal{T}_{M_1}$ such that the time-based adaptive control gain $V_{tb}(M_1 T_a) = V_M^{M_1}$ will be dominating the actual upper bound of $|\eta(\tau)|$, in accordance with (46), as

$$V_M^{M_1} \geq \Phi|\eta(\tau_1)|, \quad \tau_1 \in \mathcal{T}_{M_1}. \tag{47}$$

Starting from the end of the time interval $\mathcal{T}_{M_1}$, the process of reducing the control gain is activated, i.e., $V_M^{M_1+\ell} = V_M^{M_1+\ell-1} - \Lambda T_a$, $\ell = 1, 2, \ldots$. Thus, the dominance over the uncertainties [formalized by condition (47)] will be lost after a finite number of intervals, and there is $M_2 > M_1$ such that at $k = M_2$, the real-sliding criterion (37) will be violated. It implies that along the preceding time interval $\mathcal{T}_{M_2-1}$, a dominance inequality analogous to (47) holds

$$V_M^{M_1} \geq \Phi|\eta(\tau_2)|, \quad \tau_2 \in \mathcal{T}_{M_2-1}. \tag{48}$$

By Lemma 1, along the time interval $\mathcal{T}_{M_2-1}$, the variables z_1 and z_2 are bounded as in (38) with

$$\rho_1 = \sup_{t \in \mathcal{T}_{M_2-1}} |\dot{z}_2(t)| = G_M\big[N_{M_2-1} + V_M^{M_2-1}\big]. \tag{49}$$

Along the interval $\mathcal{T}_{M_2+1}$, i.e., one interval after the violation of the two-sliding criterion (37), the magnitude of the uncertainty $\eta(t)$ will be such that

$$|\eta(\tau_3)| \leq |\eta(\tau_2)| + 3PT \quad \forall \tau_3 \in \mathcal{T}_{M_2+1} \tag{50}$$

which is derived by taking into account (40). On the other hand, the adaptive magnitude will be increased at the end of the interval $\mathcal{T}_{M_2} - 1$ and decreased at the end of the successive interval $\mathcal{T}_{M_2+1}$, which means that

$$V_M^{M_2+1} > V_M^{M_2-1} + T(\Gamma - \Lambda). \tag{51}$$

Therefore, considering (48), (50), and (51), if the Γ parameter is such that

$$\Gamma > \Lambda + 3P \tag{52}$$

it follows that the dominance condition (46) will be already restored along the interval $\mathcal{T}_{M_2+1}$, i.e., one interval after the violation of the SM existence criterion (37). While V_M^k continues to grow, which will happen for a finite number of adaptation intervals until the SM existence criterion (37) will be restored, contractive rotations of the system trajectories in the $z_1 - z_2$ plane will take place, which can be evaluated by studying the piecewise parabolic limit trajectories of the Suboptimal algorithm (see [38]) starting from the initial condition (38). Lengthy but straightforward computations show that the transient deviations of z_1 and z_2 fulfill inequalities analogous to (42), with the constants b_1 and b_2 independent of T. The process of loosing and successively restoring the dominance over the uncertainties will iteratively continue, thereby preserving inequalities (42). Theorem 1 is proved. $\triangle$

Appendix B
Induction Generator Full-Order Dynamical Model

The four nonlinear differential equations that together with (2) describe an induction generator in a synchronously rotating direct–quadrature (d-q) frame are

$$v = \mathbf{Z} i$$

$$\mathbf{Z} = \begin{bmatrix} R_s + L_s\frac{d}{dt} & -\omega_s L_s & L_m\frac{d}{dt} & -\omega_s L_m \\ \omega_s & R_s + L_s\frac{d}{dt} & \omega_s L_m & L_m\frac{d}{dt} \\ L_m\frac{d}{dt} & -s\omega_s L_m & R_r + L_r\frac{d}{dt} & -s\omega_s L_r \\ s\omega_s L_m & L_m\frac{d}{dt} & s\omega_s L_r & R_r + L_r\frac{d}{dt} \end{bmatrix} \tag{53}$$

where $v = [v_{ds}; v_{qs}; v_{dr}; v_{qr}]^T$, $i = [i_{sd}; i_{sq}; i_{rd}; i_{rq}]^T$, (d/dt) is the time derivative operator, and L_m is the magnetizing inductance. All the rotor variables have been referred to the stator side by n_1. The equation for the generator torque, which replaces (5), is

$$T_g = p_p L_m (i_{sq} i_{rd} - i_{sd} i_{rq}). \tag{54}$$

Variables are referred to the fast shaft side by

$$T_t = \frac{T_{t\text{low}}}{k_{gb}}; \quad \Omega_g = \Omega_{\text{low}} k_{gb}; \quad J = \frac{J_t}{k_{gb}^2} + J_g \tag{55}$$

where J_t and J_g are the inertia of the turbine rotor and the generator rotating parts, respectively.

Appendix C
Parameters of the DFIG Bidirectional Topology

See Table II.

TABLE II
NOMINAL PARAMETERS OF THE DFIG BIDIRECTIONAL TOPOLOGY

P_r=37 kW;	R=7.3 m;	c_0=-0.1380;
ω_s=2π60 $\frac{\text{rad}}{\text{s}}$;	J=3.662 kgm^2;	c_1=0.0692;
V_s=375.6 V;	k_{gb}=25;	c_2=-0.0074;
p_p=2;	L_s=35.5 mH;	c_3=2.113 10^{-4};
R_s=82 mΩ;	L_r=35.5 mH;	λ_{opt}=7.63;
R_r=228 mΩ;	L_m=35.7 mH;	$C_{p\,\max}$=0.4018;

References

[1] S. Gsänger and J. Pitteloud, "Small wind world report 2014," World Wind Energy Assoc., Bonn, Germany, Tech. Rep., Mar. 2014.

[2] I. Munteanu, A. I. Bratcu, N.-A. Cutululis, and E. Ceanga, *Optimal Control of Wind Energy Systems*. London, U.K.: Springer-Verlag, 2007.

[3] M. Garcia-Sanz and C. H. Houpis, *Wind Energy Systems: Control Engineering Design*. Boca Raton, FL, USA: CRC Press, 2012.

[4] S. V. Emelyanov, *Variable-Structure Control Systems*. Moscow, Russia: Nauka, 1967.

[5] V. Utkin, "Variable structure systems with sliding modes," *IEEE Trans. Autom. Control*, vol. 22, no. 2, pp. 212–222, Apr. 1977.

[6] A. Sabanovic, L. M. Fridman, and S. K. Spurgeon, Eds., *Variable Structure Systems: From Principles to Implementation*. London, U.K.: IET, 2004.

[7] C. Edwards, E. Fossas Colet, and L. Fridman, Eds., *Advances in Variable Structure and Sliding Mode Control*. Berlin, Germany: Springer, 2006.

[8] G. Bartolini, L. Fridman, A. Pisano, and E. Usai, Eds., *Modern Sliding Mode Control Theory: New Perspectives and Applications*, vol. 375. Berlin, Germany: Springer-Verlag, 2008.

[9] Y. Shtessel, C. Edwards, L. Fridman, and A. Levant, Eds., *Sliding Mode Control and Observation*. New York, NY, USA: Springer, 2013.

This article has been accepted for inclusion in a future issue of this journal. Content is final as presented, with the exception of pagination.

[10] A. Levant, "Sliding order and sliding accuracy in sliding mode control," *Int. J. Control*, vol. 58, no. 6, pp. 1247–1263, Dec. 1993.

[11] L. Fridman and A. Levant, "Higher order sliding modes as a natural phenomenon in control theory," in *Robust Control via Variable Structure and Lyapunov Techniques*, vol. 217. London, U.K.: Springer-Verlag, 1996, ch. 1, pp. 107–133.

[12] G. Bartolini, A. Ferrara, A. Levant, and E. Usai, "On second order sliding mode controllers," in *Variable Structure Systems, Sliding Mode and Nonlinear Control*. London, U.K.: Springer, 1999, ch. 17, pp. 329–350.

[13] A. Pisano and E. Usai, "Sliding mode control: A survey with applications in math," *Math. Comput. Simul.*, vol. 81, no. 5, pp. 954–979, 2011.

[14] H. Lee and V. I. Utkin, "Chattering suppression methods in sliding mode control systems," *Annu. Rev. Control*, vol. 31, no. 2, pp. 179–188, 2007.

[15] F. Plestan, Y. Shtessel, V. Brégeault, and A. Poznyak, "New methodologies for adaptive sliding mode control," *Int. J. Control*, vol. 83, no. 9, pp. 1907–1919, 2010.

[16] Y. B. Shtessel, J. A. Moreno, F. Plestan, L. M. Fridman, and A. S. Poznyak, "Super-twisting adaptive sliding mode control: A Lyapunov design," in *Proc. 49th IEEE Conf. Decision Control (CDC)*, Dec. 2010, pp. 5109–5113.

[17] T. Gonzalez, J. A. Moreno, and L. Fridman, "Variable gain super-twisting sliding mode control," *IEEE Trans. Autom. Control*, vol. 57, no. 8, pp. 2100–2105, Aug. 2013.

[18] C. Evangelista, P. Puleston, F. Valenciaga, and L. M. Fridman, "Lyapunov-designed super-twisting sliding mode control for wind energy conversion optimization," *IEEE Trans. Ind. Electron.*, vol. 60, no. 2, pp. 538–545, Feb. 2013.

[19] C. Evangelista, F. Valenciaga, and P. Puleston, "Active and reactive power control for wind turbine based on a MIMO 2-sliding mode algorithm with variable gains," *IEEE Trans. Energy Convers.*, vol. 28, no. 3, pp. 682–689, Sep. 2013.

[20] V. I. Utkin and A. S. Poznyak, "Adaptive sliding mode control with application to super-twist algorithm: Equivalent control method," *Automatica*, vol. 49, no. 1, pp. 39–47, Jan. 2013.

[21] C. Edwards and Y. Shtessel, "Dual-layer adaptive sliding mode control," in *Proc. Amer. Control Conf. (ACC)*, Jun. 2014, pp. 4524–4529.

[22] C. Edwards and Y. Shtessel, "Adaptive dual layer second-order sliding mode control and observation," in *Proc. Amer. Control Conf. (ACC)*, Jul. 2015, pp. 5853–5858.

[23] Y. B. Shtessel, F. Plestan, and M. Taleb, "Lyapunov design of adaptive super-twisting controller applied to a pneumatic actuator," in *Proc. IFAC World Congr.*, 2011, pp. 3051–3056.

[24] Y. Shtessel, M. Taleb, and F. Plestan, "A novel adaptive-gain supertwisting sliding mode controller: Methodology and application," *Automatica*, vol. 48, no. 5, pp. 759–769, 2012.

[25] Y. Shtessel, J. Kochalummootti, C. Edwards, and S. Spurgeon, "Continuous adaptive finite reaching time control and second-order sliding modes," *IMA J. Math. Control Inf.*, vol. 30, pp. 97–113, Mar. 2013.

[26] A. Levant, M. Taleb, and F. Plestan, "Twisting-controller gain adaptation," in *Proc. 50th IEEE Conf. Decision Control Eur. Control Conf. (CDC-ECC)*, Dec. 2011, pp. 7015–7020.

[27] F. Plestan, Y. Shtessel, V. Brégeault, and A. Poznyak, "Sliding mode control with gain adaptation—Application to an electropneumatic actuator," *Control Eng. Pract.*, vol. 21, no. 5, pp. 679–688, 2013.

[28] G. Liu, A. Zinober, Y. Shtessel, and Q. Niu, "Adaptive twisting sliding mode control for the output tracking of time-delay system," *Austral. J. Elect. Electron. Eng.*, vol. 9, no. 3, pp. 217–224, 2012.

[29] J. Kochalummoottil, Y. B. Shtessel, J. A. Moreno, and L. Fridman, "Adaptive twist sliding mode control: A Lyapunov design," in *Proc. 50th IEEE Conf. Decision Control Eur. Control Conf. (CDC-ECC)*, Dec. 2011, pp. 7623–7628.

[30] J. Kochalummoottil, Y. B. Shtessel, J. A. Moreno, and L. Fridman, "Output feedback adaptive twisting control: A Lyapunov design," in *Proc. Amer. Control Conf. (ACC)*, Jun. 2012, pp. 6172–6177.

[31] G. Bartolini, A. Levant, E. Usai, and A. Pisano, "2-sliding mode with adaptation," in *Proc. 7th IEEE Medit. Conf. Control Syst.*, Haifa, Israel, 1999, pp. 2421–2429.

[32] L. Capisani, A. Ferrara, and A. Pisano, "Second-order sliding mode control with adaptive control authority for the tracking control of robotic manipulators," in *Proc. 18th IFAC World Congr.*, Milan, Italy, 2011, pp. 10319–10324.

[33] A. Pisano, M. Tanelli, and A. Ferrara, "Time-based switched sliding mode control for yaw rate regulation in two-wheeled vehicles," in *Proc. IEEE 51st Annu. Conf. Decision Control (CDC)*, Dec. 2012, pp. 5028–5033.

[34] A. Pisano, M. Tanelli, and A. Ferrara, "Combined switched/time-based adaptation in second order sliding mode control," in *Proc. IEEE 52nd Annu. Conf. Decision Control (CDC)*, Dec. 2013, pp. 4272–4277.

[35] C. Evangelista, A. Pisano, P. Puleston, and E. Usai, "Time-based adaptive second order sliding mode controller for wind energy conversion optimization," in *Proc. IEEE 53rd Annu. Conf. Decision Control (CDC)*, Los Angeles, CA, USA, Dec. 2014, pp. 2038–2043.

[36] T. Burton, D. Sharpe, N. Jenkins, and E. Bossanyi, *Wind Energy Handbook*. Chichester, U.K.: Wiley, 2001.

[37] I. Erlich and F. Shewarega, "Modeling of wind turbines equipped with doubly-fed induction machines for power system stability studies," in *Proc. IEEE PES Power Syst. Conf. Expo.*, Oct./Nov. 2006, pp. 978–985.

[38] G. Bartolini, A. Ferrara, A. Pisano, and E. Usai, "On the convergence properties of a 2-sliding control algorithm for non-linear uncertain systems," *Int. J. Control*, vol. 74, no. 7, pp. 718–731, 2001.

[39] A. Levant, "Variable measurement step in 2-sliding control," *Kybernetika*, vol. 36, no. 1, pp. 77–93, 2000.

Carolina A. Evangelista received the Engineering degree in electronics and the Ph.D. degree from the Universidad Nacional de La Plata (UNLP), La Plata, Argentina, in 2006 and 2012, respectively.

She has been a Researcher with the LEICI Instituto de Investigaciones en Electrónica, Control y Procesamiento de Señales, UNLP and Consejo Nacional de Investigaciones Científicas y Técnicas (CONICET), La Plata, Argentina, since 2013. She is currently a Professor teaching control theory with the Information Systems Engineering Department, Universidad Tecnologica Nacional, Buenos Aires, and a Teaching Assistant in Control and Automation with the Department of Electrical Engineering, UNLP. Her current research interests include high order sliding mode control, with applications in renewable energy systems (mainly wind, fuel cells, and marine waves based) and, lately, in mechanical lung ventilation.

Alessandro Pisano (M'06) was born in 1972. He received the Degree in electronics engineering and the Ph.D. degree in electronics and computer science from the Department of Electrical and Electronic Engineering, University of Cagliari, Cagliari, Italy, in 1997 and 2000, respectively.

He has spent long-term visiting periods at universities and research centers in Belgium, France, Serbia, and Mexico. He is currently an Assistant Professor with the Department of Electrical and Electronic Engineering, University of Cagliari. He is a Registered Professional Engineer in Cagliari. He has authored or co-authored one book, 62 journal publications, ten book chapters, and in excess of 100 papers in peer-reviewed international conference proceedings. He holds four patents. His current research interests include nonlinear control theory and its application to control, observation, and fault detection of nonlinear, uncertain, and/or distributed parameter systems.

Prof. Pisano is an Associate Editor of the *Asian Journal of Control* and is on the Conference Editorial Board of the IEEE Control Systems Society.

This article has been accepted for inclusion in a future issue of this journal. Content is final as presented, with the exception of pagination.

Paul Puleston received the Electronic Engineering (Hons.) and Ph.D. degrees from the Universidad Nacional de La Plata (UNLP), La Plata, Argentina, in 1988 and 1997, respectively.

He is currently a Full Professor with the Department of Electrical Engineering, Facultad de Ingeniería, UNLP, the Vice Director of the LEICI Instituto de Investigaciones en Electrónica, Control y Procesamiento de Señales, UNLP and Consejo Nacional de Investigaciones Científicas y Técnicas (CONICET), and a Researcher with the CONICET, Argentina. His current research interests include automatic control systems and theory and applications, including alternative energy systems.

Elio Usai (M'96) received the M.Sc. degree in electrical engineering from the University of Cagliari, Cagliari, Italy, in 1985.

He was a Process Engineer and then a Production Manager for international companies. In 1994, he joined the Department of Electrical and Electronic Engineering, University of Cagliari, where he is currently a Professor. He has been the Leader of research projects on the control of uncertain systems and on the model-based fault detection. He has co-authored over 150 articles in international journals and conference proceedings. His current research interests include output-feedback control, state estimation, and Fault Detection and Isolation through higher order sliding modes in linear, nonlinear, and infinite dimensional systems.

Prof. Usai was the General Chairperson of the 2006 International Workshop on Variable Structure Systems. He is an Associate Editor of the *Asian Journal of Control*, the IEEE TRANSACTIONS ON CONTROL SYSTEMS TECHNOLOGY, and the *Journal of The Franklin Institute*.